

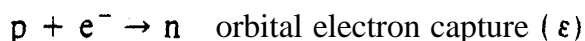
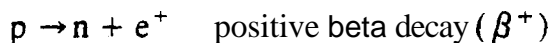
# BETA DECAY

The emission of ordinary negative electrons from the nucleus was among the earliest observed radioactive decay phenomena. The inverse process, capture by a nucleus of an electron from its atomic orbital, was not observed until 1938 when Alvarez detected the characteristic X rays emitted in the filling of the vacancy left by the captured electron. The Joliot-Curies in 1934 first observed the related process of positive electron (positron) emission in radioactive decay, only two years after the positron had been discovered in cosmic rays. These three nuclear processes are closely related and are grouped under the common name *beta* ( $\beta$ ) *decay*.

The most basic  $\beta$  decay process is the conversion of a proton to a neutron or of a neutron into a proton. In a nucleus,  $\beta$  decay changes both  $Z$  and  $N$  by one unit:  $Z \rightarrow Z \pm 1$ ,  $N \rightarrow N \mp 1$  so that  $A = Z + N$  remains constant. Thus  $\beta$  decay provides a convenient way for an unstable nucleus to “slide down” the mass parabola (Figure 3.18, for example) of constant  $A$  and to approach the stable isobar.

In contrast with a decay, progress in understanding  $\beta$  decay has been achieved at an extremely slow pace, and often the experimental results have created new puzzles that challenged existing theories. Just as Rutherford’s early experiments showed a particles to be identical with  ${}^4\text{He}$  nuclei. other early experiments showed the negative  $\beta$  particles to have the same electric charge and charge-to-mass ratio as ordinary electrons. In Section 1.2. we discussed the evidence against the presence of electrons as nuclear constituents, and so we must regard the  $\beta$  decay process as “creating” an electron from the available decay energy at the instant of decay; this electron is then immediately ejected from the nucleus. This situation contrasts with a decay, in which the  $\alpha$  particle may be regarded as having a previous existence in the nucleus.

The basic decay processes are thus:



These processes are not complete. for there is yet another particle (a neutrino or antineutrino) involved in each. The latter two processes occur only for protons

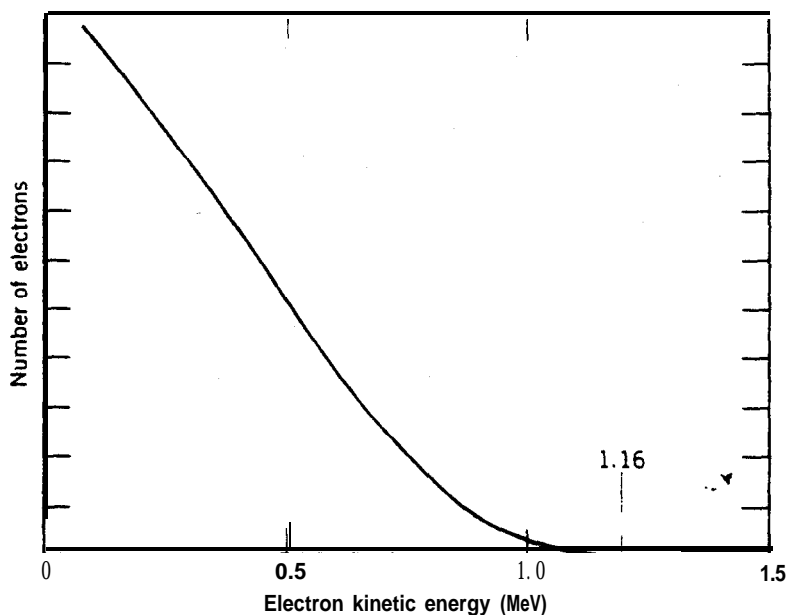


Figure 9.1 The continuous electron distribution from the  $\beta$  decay of  $^{210}\text{Bi}$  (also called RaE in the literature).

bound in nuclei; they are energetically forbidden for free protons or for protons in hydrogen atoms.

### 9.1 ENERGY RELEASE IN $\beta$ DECAY

The continuous energy distribution of the  $\beta$ -decay electrons was a confusing experimental result in the 1920s. Alpha particles are emitted with sharp, well-defined energies, equal to the difference in mass energy between the initial and final states (less the small recoil corrections); all decays connecting the same initial and final states have exactly the same kinetic energies. Beta particles have a continuous distribution of energies, from zero up to an upper limit (the endpoint energy) which is equal to the energy difference between the initial and final states. If  $\beta$  decay were, like a decay, a two-body process, we would expect all of the  $\beta$  particles to have a unique energy, but virtually all of the emitted particles have a smaller energy. For instance, we might expect on the basis of nuclear mass differences that the  $\beta$  particles from  $^{210}\text{Bi}$  would be emitted with a kinetic energy of 1.16 MeV, yet we find a continuous distribution from 0 up to 1.16 MeV (Figure 9.1).

An early attempt to account for this “missing” energy hypothesized that the  $\beta$ 's are actually emitted with 1.16 MeV of kinetic energy, but lose energy, such as by collisions with atomic electrons, before they reach the detection system. Such a possibility was eliminated by very precise calorimetric experiments that confined a  $\beta$  source and measured its decay energy by the heating effect. If a portion of the energy were transferred to the atomic electrons, a corresponding rise in temperature should be observed. These experiments showed that the shape of the spectrum shown in Figure 9.1 is a characteristic of the decay electrons themselves and not a result of any subsequent interactions.

To account for this energy release, Pauli in 1931 proposed that there was emitted in the decay process a second particle, later named by Fermi the

*neutrino*. The neutrino carries the “missing” energy and, because it is highly penetrating radiation, it is not stopped within the calorimeter, thus accounting for the failure of those experiments to record its energy. Conservation of electric charge requires the neutrino to be electrically neutral, and angular momentum conservation and statistical considerations in the decay process require the neutrino to have (like the electron) a spin of  $\frac{1}{2}$ . Experiment shows that there are in fact two different kinds of neutrinos emitted in  $\beta$  decay (and yet other varieties emitted in other decay processes; see Chapter 18). These are called the *neutrino* and the *antineutrino* and indicated by  $\nu$  and  $\bar{\nu}$ . It is the antineutrino which is emitted in  $\beta^-$  decay and the neutrino which is emitted in  $\beta^+$  decay and electron capture. In discussing  $\beta$  decay, the term “neutrino” is often used to refer to both neutrinos and antineutrinos, although it is of course necessary to distinguish between them in writing decay processes; the same is true for “electron.”

To demonstrate  $\beta$ -decay energetics we first consider the decay of the free neutron (which occurs with a half-life of about 10 min),



As we did in the case of a decay, we define the  $Q$  values to be the difference between the initial and final *nuclear mass energies*.

$$Q = (m_n - m_p - m_e - m_{\bar{\nu}})c^2 \quad (9.1)$$

and for decays of neutrons at rest,

$$Q = T_p + T_e + T_{\bar{\nu}} \quad (9.2)$$

For the moment we will ignore the proton recoil kinetic energy  $T_p$ , which amounts to only 0.3 keV. The antineutrino and electron will then share the decay energy, which: accounts for the continuous electron spectrum. The maximum-energy electrons correspond to minimum-energy antineutrinos, and when the antineutrinos have vanishingly small energies,  $Q \approx (T_e)_{\max}$ . The measured maximum energy of the electrons is  $0.782 \pm 0.013$  MeV. Using the measured neutron, electron, and proton masses, we can compute the  $Q$  value:

$$\begin{aligned} Q &= m_n c^2 - m_p c^2 - m_e c^2 - m_{\bar{\nu}} c^2 \\ &= 969.573 \text{ MeV} - 938.280 \text{ MeV} - 0.511 \text{ MeV} - m_{\bar{\nu}} c^2 \\ &= 0.782 \text{ MeV} - m_{\bar{\nu}} c^2 \end{aligned}$$

Thus to within the precision of the measured maximum energy (about 13 keV) we may regard the antineutrino as massless. Other experiments provide more stringent upper limits, as we discuss in Section 9.6, and for the present discussion we take the masses of the neutrino and antineutrino to be identically zero.

Conservation of linear momentum can be used to identify  $\beta$  decay as a three-body process, but this requires measuring the momentum of the recoiling nucleus in coincidence with the momentum of the electron. These experiments are difficult, for the low-energy nucleus ( $T \lesssim \text{keV}$ ) is easily scattered, but they have been done in a few cases, from which it can be deduced that the vector sum of the linear momenta of the electron and the recoiling nucleus is consistent with an unobserved third particle carrying the “missing” energy and having a rest mass of zero or nearly zero. Whatever its mass might be, the existence of the

additional particle is absolutely required by these experiments. for the momenta of the electron and nucleus certainly do not sum to zero. as they would in a two-body decay.

Because the neutrino is massless, it moves with the speed of light and its total relativistic energy  $E_\nu$  is the same as its kinetic energy; we will use  $E_\nu$  to represent neutrino energies. (A review of the concepts and formulas of relativistic kinematics may be found in Appendix A.) For the electron, we will use both its kinetic energy  $T_e$  and its total relativistic energy  $E_e$ , which are of course related by  $E_e = T_e + m_e c^2$ . (Decay energies are typically of order MeV; thus the nonrelativistic approximation  $T \ll mc^2$  is certainly not valid for the decay electrons. and we *must* use relativistic kinematics.) The nuclear recoil is of very low energy and can be treated nonrelativistically.

Let's consider a typical negative  $\beta$ -decay process in a nucleus:

$${}^A_Z X_N \rightarrow {}^A_{Z+1} X'_{N-1} + e^- + \bar{\nu} \quad (9.3)$$

$$Q_{\beta^-} = [m_N({}^A_Z X) - m_N({}^A_{Z+1} X') - m_e] c^2$$

where  $m_N$  indicates *nuclear* masses. To convert nuclear masses into the tabulated neutral atomic mass+, which we denote as  $m({}^A_Z X)$ , we use

$$m({}^A_Z X) c^2 = m_N({}^A_Z X) c^2 + Z m_e c^2 - \sum_{i=1}^Z B_i \quad (9.4)$$

where  $B_i$  represents the binding energy of the  $i$ th electron. In terms of atomic masses,

$$Q_{\beta^-} = \{ [m({}^A_Z X) - Z m_e] - [m({}^A_{Z+1} X') - (Z+1) m_e] - m_e \} c^2$$

$$+ \left\{ \sum_{i=1}^Z B_i - \sum_{i=1}^{Z+1} B_i \right\} \quad (9.5)$$

Notice that the electron masses cancel in this case. Neglecting the differences in electron binding energy, we therefore find

$$Q_{\beta^-} = [m({}^A_Z X) - m({}^A_{Z+1} X')] c^2 \quad (9.6)$$

where the masses are neutral atomic masses. The  $Q$  value represents the energy shared by the electron and neutrino:

$$Q_{\beta^-} = T_e + E_{\bar{\nu}} \quad (9.7)$$

and it follows that each has its maximum when the other approaches zero:

$$(T_e)_{\max} = (E_{\bar{\nu}})_{\max} = Q_{\beta^-} \quad (9.8)$$

In the case of the  ${}^{210}\text{Bi} \rightarrow {}^{210}\text{Po}$  decay, the mass tables give

$$Q_{\beta^-} = [m({}^{210}\text{Bi}) - m({}^{210}\text{Po})] c^2$$

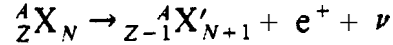
$$= (209.984095 \text{ u} - 209.982848 \text{ u})(931.502 \text{ MeV/u})$$

$$= 1.161 \text{ MeV}$$

Figure 9.1 showed  $(T_e)_{\max} = 1.16 \text{ MeV}$ , in agreement with the value expected from  $Q_{\beta^-}$ . Actually, this is really not an agreement between two independent values. The value of  $Q_{\beta^-}$  is used in this case to *determine* the mass of  ${}^{210}\text{Po}$ , with

the mass of  $^{210}\text{Bi}$  determined from that of  $^{209}\text{Bi}$  using neutron capture. Equation 9.6 is used with the measured  $Q_{\beta^-}$  to obtain  $m(^4\text{X}')$ .

In the case of positron decay, a typical decay process is

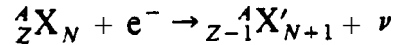


and a calculation similar to the previous one shows

$$Q_{\beta^+} = [m(^4\text{X}) - m(^4\text{X}') - 2m_e]c^2 \quad (9.9)$$

again using *atomic* masses. Notice that the electron masses *do not* cancel in this case.

For electron-capture processes, such as



the calculation of the  $Q$  value must take into account that the atom  $\text{X}'$  is in an *atomic* excited state immediately after the capture. That is, if the capture takes place from an inner shell, the K shell for instance, an electronic vacancy in that shell results. The vacancy is quickly filled as electrons from higher shells make downward transitions and emit characteristic X rays. Whether one X ray is emitted or several, the total X-ray energy is equal to the binding energy of the captured electron. Thus the atomic mass of  $\text{X}'$  immediately after the decay is greater than the mass of  $\text{X}'$  in its atomic ground state by  $B_n$ , the binding energy of the captured  $n$ -shell electron ( $n = \text{K, L, } \dots$ ). The  $Q$  value is then

$$Q_e = [m(^4\text{X}) - m(^4\text{X}')]c^2 - B_n \quad (9.10)$$

Positive  $\beta^+$  decay and electron capture both lead from the initial nucleus  ${}_Z^AX_N$  to the final nucleus  ${}_{Z-1}^AX'_{N+1}$ , but note that both may not always be energetically possible ( $Q$  must be positive for any decay process). Nuclei for which  $\beta^+$  decay is energetically possible may also undergo electron capture, but the reverse is not true—it is possible to have  $Q > 0$  for electron capture while  $Q < 0$  for  $\beta^+$  decay. The atomic mass energy difference must be at least  $2m_e c^2 = 1.022 \text{ MeV}$  to permit  $\beta^+$  decay.

In positron decay, expressions of the form of Equations 9.7 and 9.8 show that there is a continuous distribution of neutrino energies up to  $Q_{\beta^+}$  (less the usually negligible nuclear recoil). In electron capture, however, the two-body final state results in unique values for the recoil energy and  $E_\nu$ . Neglecting the recoil, a monoenergetic neutrino with energy  $Q_e$  is emitted.

All of the above expressions refer to decays between nuclear ground states. If the final nuclear state  $\text{X}'$  is an excited state, the  $Q$  value must be accordingly

**Table 9.1 Typical  $\beta$ -Decay Processes**

Decay	Type	$Q$ (MeV)	$t_{1/2}$
$^{23}\text{Ne} \rightarrow ^{23}\text{Na} + e^- + \bar{\nu}$	$\beta^-$	4.38	38 s
$^{99}\text{Tc} \rightarrow ^{99}\text{Ru} + e^- + \bar{\nu}$	$\beta^-$	0.29	$2.1 \times 10^5 \text{ y}$
$^{25}\text{Al} \rightarrow ^{25}\text{Mg} + e^+ + \nu$	$\beta^+$	3.26	7.2 s
$^{124}\text{I} \rightarrow ^{124}\text{Te} + e^+ + \nu$	$\beta^+$	2.14	4.2 d
$^{15}\text{O} + e^- \rightarrow ^{15}\text{N} + \nu$	$\epsilon$	2.75	1.22 s
$^{41}\text{Ca} + e^- \rightarrow ^{41}\text{K} + \nu$	$\epsilon$	0.43	$1.0 \times 10^5 \text{ y}$

decreased by the excitation energy of the state:

$$Q_{\text{ex}} = Q_{\text{ground}} - E_{\text{ex}} \quad (9.11)$$

Table 9.1 shows some typical  $\beta$  decay processes, their energy releases, and their half-lives.

## 9.2 FERMI THEORY OF $\beta$ DECAY

In our calculation of  $\alpha$ -decay half-lives in Chapter 8, we found that the barrier penetration probability was the critical factor in determining the half-life. In negative  $\beta$  decay there is no such barrier to penetrate and even in  $\beta^+$  decay, it is possible to show from even a rough calculation that the exponential factor in the barrier penetration probability is of order unity. There are other important differences between  $\alpha$  and  $\beta$  decay which suggest to us that we must use a completely different approach for the calculation of transition probabilities in  $\beta$  decay: (1) The electron and neutrino do not exist before the decay process, and therefore we must account for the formation of those particles. (2) The electron and neutrino must be treated relativistically. (3) The continuous distribution of electron energies must result from the calculation.

In 1934, Fermi developed a successful theory of  $\beta$  decay based on Pauli's neutrino hypothesis. The essential features of the decay can be derived from the basic expression for the transition probability caused by an interaction that is weak compared with the interaction that forms the quasi-stationary states. This is certainly true for  $\beta$  decay, in which the characteristic times (the half-lives, typically of order seconds or longer) are far longer than the characteristic nuclear time ( $10^{-20}$  s). The result of this calculation, treating the decay-causing interaction as a weak perturbation, is Fermi's Golden Rule, a general result for any transition rate previously given in Equation 2.79:

$$= \frac{2\pi}{\hbar} |V_{fi}|^2 \rho(E_f) \quad (9.12)$$

The matrix element  $V_{fi}$  is the integral of the interaction  $V$  between the initial and final quasi-stationary states of the system:

$$V_{fi} = \int \psi_f^* V \psi_i dv \quad (9.13)$$

The factor  $\rho(E_f)$  is the density of final states, which can also be written as  $dn/dE_f$ , the number  $dn$  of final states in the energy interval  $dE_f$ . A given transition is more likely to occur if there is a large number of accessible final states.

Fermi did not know the mathematical form of  $V$  for  $\beta$  decay that would have permitted calculations using Equations 9.12 and 9.13. Instead, he considered all possible forms consistent with special relativity, and he showed that  $V$  could be replaced with one of five mathematical operators  $O_X$ , where the subscript  $X$  gives the form of the operator  $O$  (that is its transformation properties):  $X = V$  (vector),  $A$  (axial vector),  $S$  (scalar),  $P$  (pseudoscalar), or  $T$  (tensor). Which of these is correct for  $\beta$  decay can be revealed only through experiments that study

the symmetries and the spatial properties of the decay products, and it took 20 years (and several mistaken conclusions) for the correct V-A form to be deduced.

The final state wave function must include not only the nucleus but also the electron and neutrino. For electron capture or neutrino capture, the forms would be similar,, but the appropriate wave function would appear in the initial state. For  $\beta$  decay, the interaction matrix element then has the form

$$V_{fi} = g \int [\psi_f^* \varphi_e^* \varphi_\nu^*] O_X \psi_i dv \quad (9.14)$$

where now  $\psi_f$  refers only to the final nuclear wave function and  $\varphi_e$  and  $\varphi_\nu$  give the wave functions of the electron and neutrino. The quantity in square brackets represents the entire final system after the decay. The value of the constant  $g$  determines the strength of the interaction; the electronic charge  $e$  plays a similar role in the interaction between an atom and the electromagnetic field.

The density of states factor determines (to lowest order) the shape of the beta energy spectrum. To find the density of states, we need to know the number of final states accessible to the decay products. Let us suppose in the decay that we have an electron (or positron) emitted with momentum  $p$  and a neutrino (or antineutrino) with momentum  $q$ . We are interested at this point only in the *shape* of the energy spectrum, and thus the directions of  $p$  and  $q$  are of no interest. If we imagine a coordinate system whose axes are labeled  $p_x, p_y, p_z$ , then the locus of the points representing a specific value of  $|p| = (p_x^2 + p_y^2 + p_z^2)^{1/2}$  is a sphere of, radius  $p = |p|$ . More specifically, the locus of points representing momenta in the range  $dp$  at  $p$  is a spherical shell of radius  $p$  and thickness  $dp$ , thus having volume  $4\pi p^2 dp$ . If the electron is confined to a box of volume  $V$  (this step is taken only for completeness and to permit the wave function to be normalized; the actual volume will cancel from the final result), then the number of final electron states  $dn_e$ , corresponding to momenta in the range  $p$  to  $p + dp$ , is

$$dn_e = \frac{4\pi p^2 dp V}{h^3} \quad (9.15)$$

where the factor  $h^3$  is included to make the result a dimensionless pure number.\* Similarly, the number of neutrino states is

$$dn_\nu = \frac{4\pi q^2 dq V}{h^3} \quad (9.16)$$

and the number of final states which have simultaneously an electron and a neutrino with the proper momenta is

$$d^2n = dn_e dn_\nu = \frac{(4\pi)^2 V^2 p^2 dp q^2 dq}{h^6} \quad (9.17)$$

\*The available spatial and momentum states are counted in six-dimensional  $(x, y, z, p_x, p_y, p_z)$  phase space: the unit volume in phase space is  $h^3$ .

The electron and neutrino wave functions have the usual free-particle form, normalized within the volume  $V$ :

$$\begin{aligned}\varphi_e(\mathbf{r}) &= \frac{1}{\sqrt{V}} e^{i\mathbf{p}\cdot\mathbf{r}/\hbar} \\ \varphi_\nu(\mathbf{r}) &= \frac{1}{\sqrt{V}} e^{i\mathbf{q}\cdot\mathbf{r}/\hbar}\end{aligned}\quad (9.18)$$

For an electron with 1 MeV kinetic energy,  $p = 1.4$  MeV/c and  $p/\hbar = 0.007$  fm $^{-1}$ . Thus over the nuclear volume,  $pr \ll 1$  and we can expand the exponentials, keeping only the first term:

$$\begin{aligned}e^{i\mathbf{p}\cdot\mathbf{r}/\hbar} &= 1 + \frac{i\mathbf{p}\cdot\mathbf{r}}{\hbar} + \dots \cong 1 \\ e^{i\mathbf{q}\cdot\mathbf{r}/\hbar} &= 1 + \frac{i\mathbf{q}\cdot\mathbf{r}}{\hbar} + \dots \cong 1\end{aligned}\quad (9.19)$$

This approximation is known as the *allowed* approximation.

In this approximation, the only factors that depend on the electron or neutrino energy come from the density of states. Let's assume we are trying to calculate the momentum and energy distributions of the emitted electrons. The partial decay rate for electrons and neutrinos with the proper momenta is

$$d\lambda = \frac{2\pi}{\hbar} g^2 |M_{fi}|^2 (4\pi)^2 \frac{p^2 dp q^2 dq}{h^6 dE_f} \quad (9.20)$$

where  $M_{fi} = \int \psi_f^* O_X \psi_i dv$  is the *nuclear matrix element*. The final energy  $E_f$  is just  $E_e + E_\nu = E_e + qc$ , and so  $dq/dE_f = 1/c$  at fixed  $E_e$ . As far as the shape of the electron spectrum is concerned, all of the factors in Equation 9.20 that do not involve the momentum (including  $M_{fi}$ , which for the present we assume to be independent of  $p$ ) can be combined into a constant  $C$ , and the resulting distribution gives the number of electrons with momentum between  $p$  and  $p + dp$ :

$$N(p) dp = C p^2 q^2 dp \quad (9.21)$$

If  $Q$  is the decay energy, then ignoring the negligible nuclear recoil energy,

$$q = \frac{Q - T_e}{c} = \frac{Q - \sqrt{p^2 c^2 + m_e^2 c^4} + m_e c^2}{c} \quad (9.22)$$

and the spectrum shape is given by

$$N(p) = \frac{C}{c^2} p^2 (Q - T_e)^2 \quad (9.23)$$

$$= \frac{C}{c^2} p^2 \left[ Q - \sqrt{p^2 c^2 + m_e^2 c^4} + m_e c^2 \right]^2 \quad (9.24)$$

This function vanishes at  $p = 0$  and also at the endpoint where  $T_e = Q$ ; its shape is shown in Figure 9.2.



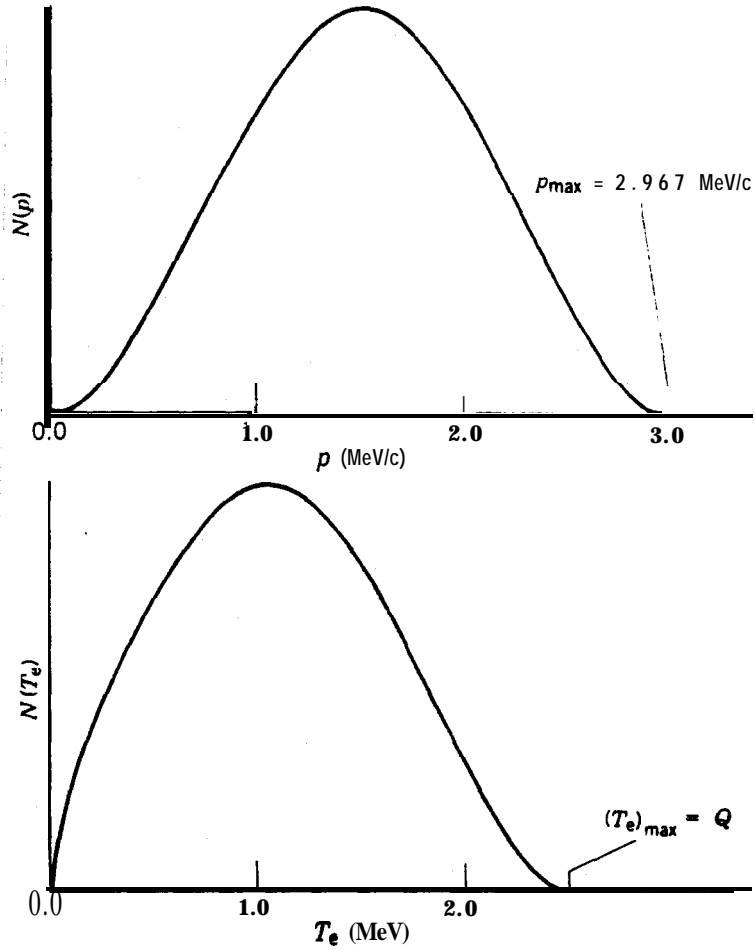


Figure 9.2 Expected electron energy and momentum distributions, from Equations 9.24 and 9.25. These distributions are drawn for  $Q = 2.5$  MeV.

More frequently we are interested in the energy spectrum, for electrons with kinetic energy between  $T_e$  and  $T_e + dT_e$ . With  $c^2 p dp = (T_e + m_e c^2) dT_e$ , we have

$$N(T_e) = \frac{C}{c^5} (T_e^2 + 2T_e m_e c^2)^{1/2} (Q - T_e)^2 (T_e + m_e c^2) \quad (9.25)$$

This distribution, which also vanishes at  $T_e = 0$  and at  $T_e = Q$ , is shown in Figure 9.2.

In Figure 9.3, the  $\beta^+$  and  $\beta^-$  decays of  $^{64}\text{Cu}$  are compared with the predictions of the theory. As you can see, the general shape of Figure 9.2 is evident, but there are systematic differences between theory and experiment. These differences originate with the Coulomb interaction between the  $\beta$  particle and the daughter nucleus. Semiclassically, we can interpret the shapes of the momentum distributions of Figure 9.3 as a Coulomb repulsion of  $\beta^+$  by the nucleus, giving fewer low-energy positrons, and a Coulomb attraction of  $\beta^-$ , giving more low-energy electrons. From the more correct standpoint of quantum mechanics, we should instead refer to the change in the electron plane wave. Equation 9.19, brought about by the Coulomb potential inside the nucleus. The quantum mechanical calculation of the effect of the nuclear Coulomb field on the electron wave function is beyond the level of this text. It modifies the spectrum by introducing an additional factor, the Fermi function  $F(Z', p)$  or  $F(Z', T_e)$ , where  $Z'$  is the atomic number of the daughter nucleus. Finally, we must

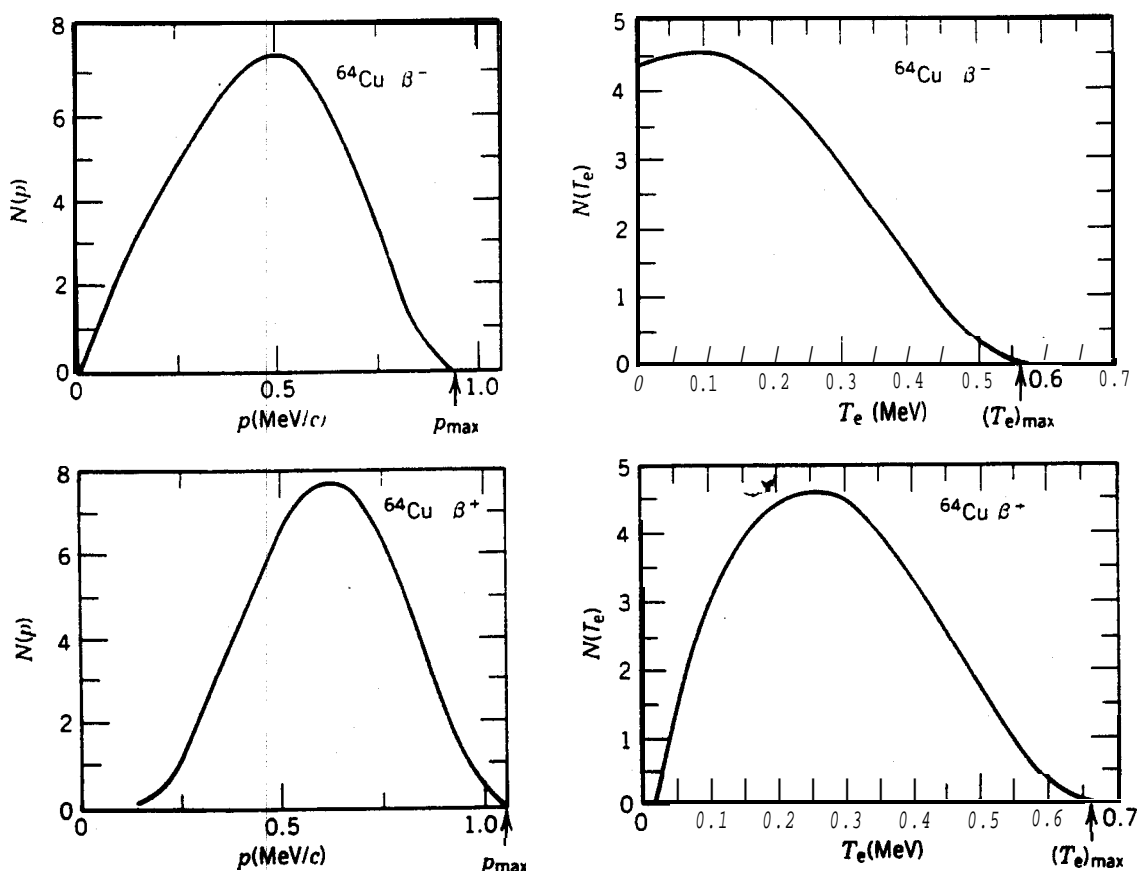


**Figure 9.8** Momentum and kinetic energy spectra of electrons and positrons emitted in the decay of  $^{64}\text{Cu}$ . Compare with Figure 9.2; the differences arise from the Coulomb interactions with the daughter nucleus. From R. D. Evans, *The Atomic Nucleus* (New York: McGraw-Hill, 1955).

consider the effect of the nuclear matrix element,  $M_{fi}$ , which we have up to now assumed not to influence the shape of the spectrum. This approximation (also called the allowed approximation) is often found to be a very good one, but there are some cases in which it is very bad—in fact, there are cases in which  $M_{fi}$  vanishes in the allowed approximation, giving no spectrum at all! In such cases, we must take the next terms of the plane wave expansion, Equations 9.19, which introduce yet another momentum dependence. Such cases are called, somewhat incorrectly, *forbidden* decays; these decays are not absolutely forbidden, but as we will learn subsequently, they are less likely to occur than allowed decays and therefore tend to have longer half-lives. The degree to which a transition is forbidden depends on how far we must take the expansion of the plane wave to find a nonvanishing nuclear matrix element. Thus the first term beyond the 1 gives first-forbidden decays, the next term gives second-forbidden, and so on. We will see in Section 9.4 how the angular momentum and parity selection rules restrict the kinds of decay that can occur.

The complete  $\beta$  spectrum then includes three factors:

1. The statistical factor  $p^2(Q - T_e)^2$ , derived from the number of final states accessible to the emitted particles.
2. The Fermi function  $F(Z', p)$ , which accounts for the influence of the nuclear Coulomb field.

3. The nuclear matrix element  $|M_{fi}|^2$ , which accounts for the effects of particular initial and final nuclear states and which may include an additional electron and neutrino momentum dependence  $S(p, q)$  from forbidden terms:

$$N(p) \propto p^2(Q - T_e)^2 F(Z', p) |M_{fi}|^2 S(p, q) \quad (9.26)$$

### 9.3 THE "CLASSICAL" EXPERIMENTAL TESTS OF THE FERMI THEORY

#### The Shape of the $\beta$ Spectrum

In the allowed approximation, we can rewrite Equation 9.26 as

$$(Q - T_e) \propto \sqrt{\frac{N(p)}{p^2 F(Z', p)}} \quad (9.27)$$

and plotting  $\sqrt{N(p)/p^2 F(Z', p)}$  against  $T_e$  should give a straight line which intercepts the x axis at the decay energy  $Q$ . Such a plot is called a *Kurie plot* (sometimes a Fermi plot or a Fermi-Kurie plot). An example of a Kurie plot is shown in Figure 9.4. The linear nature of this plot gives us confidence in the theory as it has been developed, and also gives us a convenient way to determine the decay endpoint energy (and therefore the  $Q$  value).

In the case of forbidden decays, the standard Kurie plot does not give a straight line, but we can restore the linearity of the plot if we instead graph  $\sqrt{N(p)/p^2 F(Z', p) S(p, q)}$  against  $T_e$ , where  $S$  is the momentum dependence that results from the higher-order term in the expansion of the plane wave. The function  $S$  is known as the *shape factor*; for certain first-forbidden decays, for example, it is simply  $p^2 + q^2$ .

Including the shape factor gives a linear plot, as Figure 9.5 shows.

#### The Total Decay Rate

To find the total decay rate, we must integrate Equation 9.20 over all values of the electron momentum  $p$ , keeping the neutrino momentum at the value determined by Equation 9.22, which of course also depends on  $p$ . Thus, for allowed decays,

$$\lambda = \frac{g^2 |M_{fi}|^2}{2\pi^3 \hbar^7 c^3} \int_0^{p_{\max}} F(Z', p) p^2 (Q - T_e)^2 dp \quad (9.28)$$

The integral will ultimately depend only on  $Z'$  and on the maximum electron total energy  $E_0$  (since  $cp_{\max} = \sqrt{E_0^2 - m_e^2 c^4}$ ), and we therefore represent it as

$$f(Z', E_0) = \frac{1}{(m_e c)^3 (m_e c^2)^2} \int_0^{p_{\max}} F(Z', p) p^2 (E_0 - E_e)^2 dp \quad (9.29)$$

where the constants have been included to make  $f$  dimensionless. The function  $f(Z', E_0)$  is known as the *Fermi integral* and has been tabulated for values of  $Z'$  and  $E_0$ .

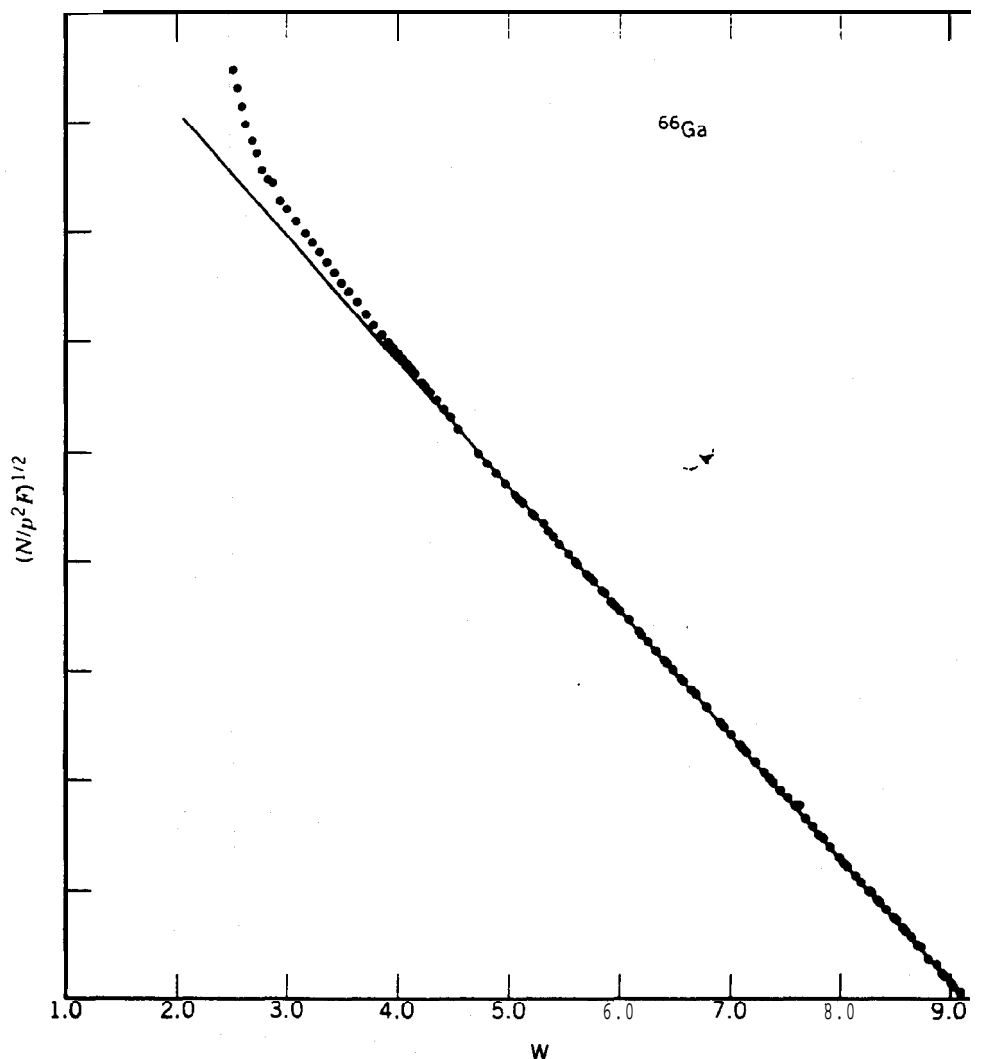


**FIGURE 9.4** Fermi - Kurie plot of allowed  $0^+ \rightarrow 0^+$  decay of  $^{66}\text{Ga}$ . The horizontal scale is the relativistic total energy  $(T_e + m_e c^2)$  in units of  $m_e c^2$ . The deviation from the straight line at low energy arises from the scattering of low-energy electrons within the radioactive source, From D. C. Camp and L. M. Langer, Phys. Rev. 129, 1782 (1963).

With  $\lambda = 0.693/t_{1/2}$ , we have

$$ft_{1/2} = 0.693 \frac{2\pi^3 \hbar^7}{g^2 m_e^5 c^4 |M_{fi}|^2} \quad (9.30)$$

The quantity on the left side of Equation 9.30 is called the *comparative half-life* or *ft value*. It gives us a way to compare the  $\beta$ -decay probabilities in different nuclei—Equation 9.28 shows that the decay rate depends on  $Z'$  and on  $E_0$ , and this dependence is incorporated into  $f$ , so that *differences in ft values must be due to differences in the nuclear matrix element* and thus to differences in the nuclear wave function.

As in the case of  $\alpha$  decay, there is an enormous range of half-lives in  $\beta$  decay— $ft$  values range from about  $10^3$  to  $10^{20}$  s. For this reason, what is often quoted is the value of  $\log_{10} ft$  (with  $t$  given in seconds). The decays with the shortest comparative half-lives ( $\log ft \approx 3$ –4) are known as *superallowed* decays. Some of

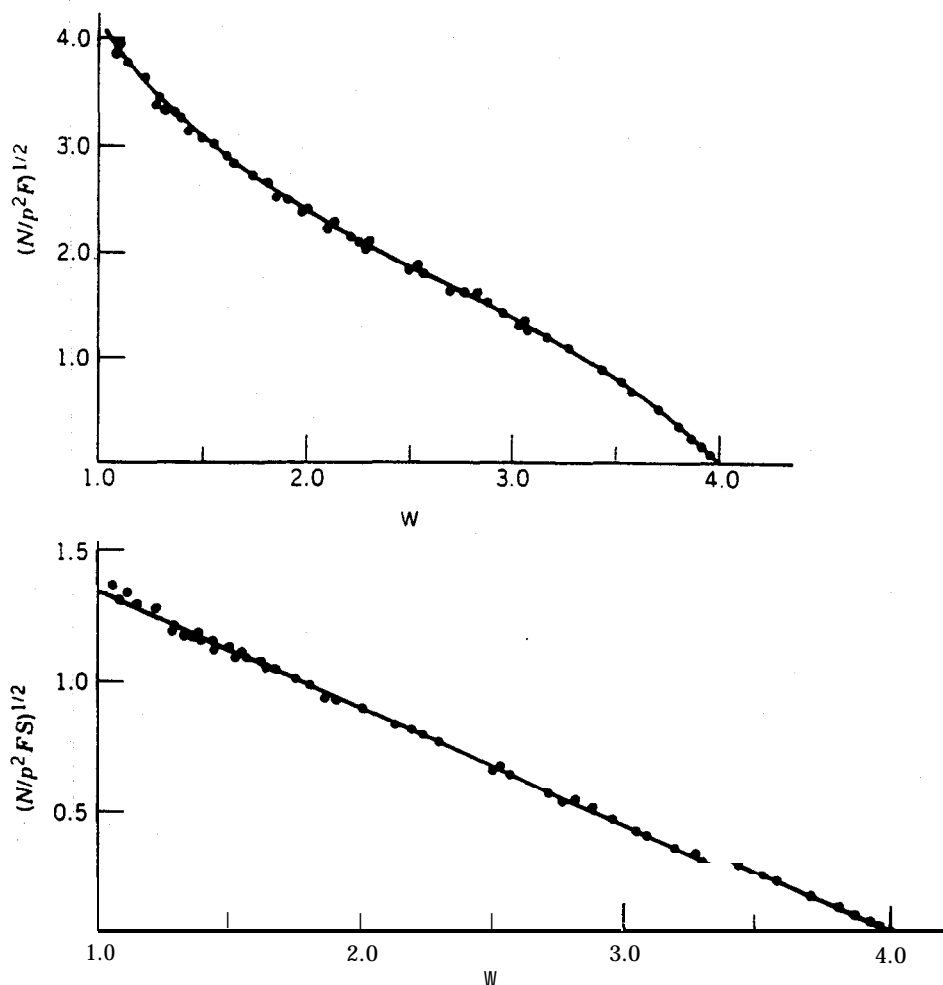


Figure 9.5 Uncorrected Fermi-Kurie plot in the  $\beta$  decay of  $^{91}\text{Y}$  (top). The linearity is restored if the shape factor  $S(p, 9)$  is included: for this type of first-forbidden decay, the shape factor  $p^2 + q^2$  gives a linear plot (bottom). Data from L. M. Langer and H. C. Price, Phys. Rev. 75, 1109 (1949).

the superallowed decays have  $0^+$  initial and final states, in which case the nuclear matrix element can be calculated quite easily:  $M_{fi} = \sqrt{2}$ . The  $\log ft$  values for  $0^+ \rightarrow 0^+$  decays should all be identical. Table 9.2 shows the  $\log ft$  values of all known  $0^+ \rightarrow 0^+$  superallowed transitions, and within experimental error the values appear to be quite constant. Moreover, with  $M_{fi} = \sqrt{2}$ , we can use Equation 9.30 to find a value of the  $g$ -decay strength constant

$$g = 0.88 \times 10^{-4} \text{ MeV} \cdot \text{fm}^3$$

To make this constant more comparable to other fundamental constants, we should express it in a dimensionless form. We can then compare it with dimensionless constants of other interactions (the fine structure constant which characterizes the electromagnetic interaction, for instance). Letting  $M$ ,  $L$ , and  $T$  represent, respectively, the dimensions of mass, length, and time, the dimensions of  $g$  are  $M^1 L^5 T^{-2}$ , and no combinations of the fundamental constants  $\hbar$  (dimension  $M^1 L^2 T^{-1}$ ) and  $c$  (dimension  $L^1 T^{-1}$ ) can be used to convert  $g$  into a dimensionless constant. (For instance,  $\hbar c^3$  has dimension  $M^1 L^5 T^{-5}$ , and so  $g/\hbar c^3$  has dimension  $T^3$ .) Let us therefore introduce an arbitrary mass  $m$  and

Table 9.2  $ft$  Values for  $0^+ \rightarrow 0^+$  Superaligned Decays

Decay	$ft$ (s)
$^{10}\text{C} \rightarrow ^{10}\text{B}$	$3100 \pm 31$
$^{14}\text{O} \rightarrow ^{14}\text{N}$	$3092 \pm 4$
$^{18}\text{Ne} \rightarrow ^{18}\text{F}$	$3084 \pm 76$
$^{22}\text{Mg} \rightarrow ^{22}\text{Na}$	$3014 \pm 78$
$^{26}\text{Al} \rightarrow ^{26}\text{Mg}$	$3081 \pm 4$
$^{26}\text{Si} \rightarrow ^{26}\text{Al}$	$3052 \pm 51$
$^{30}\text{S} \rightarrow ^{30}\text{P}$	$3120 \pm 82$
$^{34}\text{Cl} \rightarrow ^{34}\text{S}$	$3087 \pm 9$
$^{34}\text{Ar} \rightarrow ^{34}\text{Cl}$	$3101 \pm 20$
$^{38}\text{K} \rightarrow ^{38}\text{Ar}$	$3102 \pm 8$
$^{38}\text{Ca} \rightarrow ^{38}\text{K}$	$3145 \pm 138$
$^{42}\text{Sc} \rightarrow ^{42}\text{Ca}$	$3091 \pm 7$
$^{42}\text{Ti} \rightarrow ^{42}\text{Sc}$	$3275 \pm 1039$
$^{46}\text{V} \rightarrow ^{46}\text{Ti}$	$3082 \pm 13$
$^{46}\text{Cr} \rightarrow ^{46}\text{V}$	$2834 \pm 657$
$^{50}\text{Mn} \rightarrow ^{50}\text{Cr}$	$3086 \pm 8$
$^{54}\text{Co} \rightarrow ^{54}\text{Fe}$	$3091 \pm 5$
$^{62}\text{Ga} \rightarrow ^{62}\text{Zn}$	$2549 \pm 1280$

try to choose the exponents  $i$ ,  $j$ , and  $k$  so that  $g/m^i \hbar^j c^k$  is dimensionless. A solution immediately follows with  $i = -2$ ,  $j = 3$ ,  $k = -1$ . Thus the desired ratio, indicated by  $G$ , is

$$G = \frac{g}{m^{-2} \hbar^3 c^{-1}} = g \frac{m^2 c}{\hbar^3} \quad (9.31)$$

There is no clear indication of what value to use for the mass in Equation 9.31. If we are concerned with the nucleon-nucleon interaction, it is appropriate to use the nucleon mass, in which case the resulting dimensionless strength constant is  $G = 1.0 \times 10^{-5}$ . The comparable constant describing the pion-nucleon interaction, denoted by  $g_\pi^2$  in Chapter 4, is of order unity. We can therefore rank the four basic nucleon-nucleon interactions in order of strength:

pion-nucleon ("strong")	1
electromagnetic	$10^{-2}$
$\beta$ decay ("weak")	$10^{-5}$
gravitational	$10^{-39}$

(The last entry follows from a similar conversion of the universal gravitational constant into dimensionless form also using the nucleon mass.) The  $\beta$ -decay interaction is one of a general class of phenomena known collectively as *weak interactions*, all of which are characterized by the strength parameter  $g$ . The Fermi theory is remarkably successful in describing these phenomena, to the extent that they are frequently discussed as examples of the *universal Fermi*

interaction. Nevertheless, the Fermi theory fails in several respects to account for some details of the weak interaction (details which are unimportant for the present discussion of  $\beta$  decay). A theory that describes the weak interaction in terms of exchanged particles (just as the strong nuclear force was described in Chapter 4) is more successful in explaining these properties. The recently discovered exchanged particles (with the unfortunate name *intermediate vector bosons*) are discussed in more detail in Chapter 18.

### The Mass of the Neutrino

The Fermi theory is based on the *assumption* that the rest mass of the neutrino is zero. Superficially, it might seem that the neutrino rest mass would be a reasonably easy quantity to measure in order to verify this assumption. Looking back at Equations 9.1 and 9.2, or their equivalents for nuclei with  $A > 1$ , we immediately see a method to test the assumption. We can calculate the decay  $Q$  value (including a possible nonzero value of the neutrino mass) from Equations 9.6 or 9.9, and we can measure the  $Q$  value, as in Equation 9.8, from the maximum energy of the  $\beta$  particles. Comparison of these two values then permits a value for the neutrino mass to be deduced.

From this procedure we can conclude that the neutrino rest mass is smaller than about  $1 \text{ keV}/c^2$ , but we cannot extend far below that limit because the measured atomic masses used to compute  $Q$  have precisions of the order of keV, and the deduced endpoint energies also have experimental uncertainties of the order of keV. A superior method uses the shape of the  $\beta$  spectrum near the upper limit. If  $m_\nu \neq 0$  then Equation 9.22 is no longer strictly valid. However, if  $m_\nu c^2 \ll Q$ , then over most of the observed  $\beta$  spectrum  $E_\nu \gg m_\nu c^2$  and the neutrino can be treated in the extreme relativistic approximation  $E_\nu \approx pc$ . In this case, Equation 9.22 will be a very good approximation and the neutrino mass will have a negligible effect. Near the endpoint of the  $\beta$  spectrum, however, the neutrino energy approaches zero and at some point we would expect  $E_\nu \sim m_\nu c^2$ , in which case our previous calculation of the statistical factor for the spectrum shape is incorrect. Still closer to the **endpoint**, the neutrino kinetic energy becomes still smaller and we may begin to treat it nonrelativistically, so that  $q^2 = 2m_\nu T_\nu$ , and

$$N(p) \propto p^2 [Q - \sqrt{p^2 c^2 + m_\nu^2 c^4} + m_\nu c^2]^{1/2} \quad (9.32)$$

which follows from a procedure similar to that used to obtain Equation 9.24, except that for  $m_\nu > 0$  we must use  $dq/dE_\nu = m_\nu/q$  in the nonrelativistic limit. Also,

$$N(T_\nu) \propto (T_\nu^2 + 2T_\nu m_\nu c^2)^{1/2} (Q - T_\nu)^{1/2} (T_\nu + m_\nu c^2) \quad (9.33)$$

The quantity in square brackets in Equations 9.32 and 9.24, which is just  $(Q - T_\nu)$ , vanishes at the endpoint. Thus at the endpoint  $dN/dp \rightarrow 0$  if  $m_\nu = 0$ , while  $dN/dp \rightarrow \infty$  if  $m_\nu > 0$ . That is, the momentum spectrum approaches the

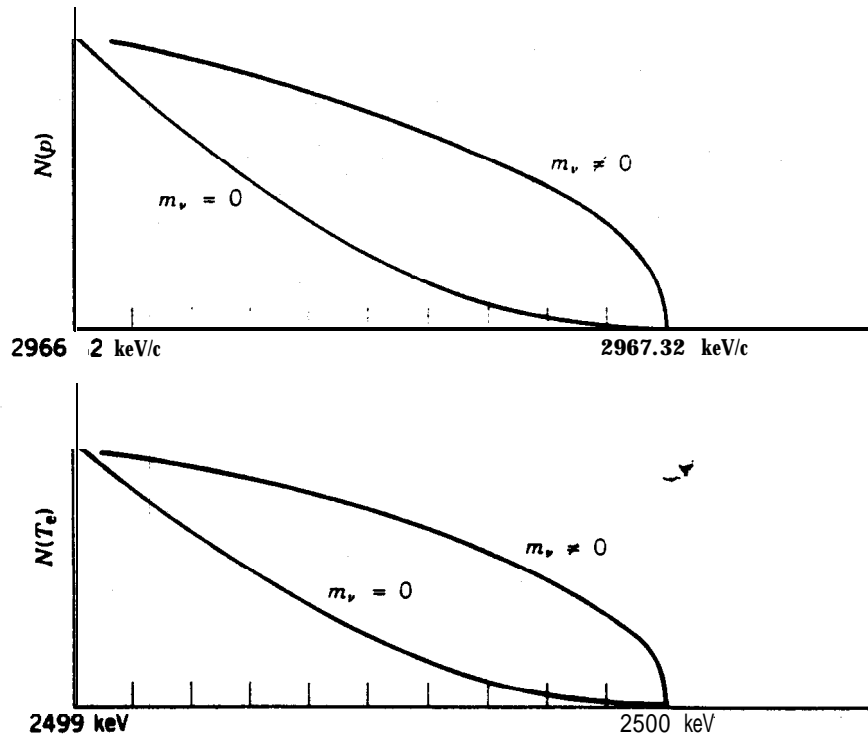


Figure 9.6 Expanded view of the upper 1-keV region of the momentum and energy spectra of Figure 9.2. The normalizations are arbitrary; what is significant is the difference in the shape of the spectra for  $m_\nu = 0$  and  $m_\nu \neq 0$ . For  $m_\nu = 0$ , the slope goes to zero at the endpoint; for  $m_\nu \neq 0$ , the slope at the endpoint is infinite.

endpoint with zero slope for  $m_\nu = 0$  and with infinite slope for  $m_\nu > 0$ . The slope of the energy spectrum,  $dN/dT_e$ , behaves identically. We can therefore study the limit on the neutrino mass by looking at the slope at the endpoint of the spectrum, as suggested by Figure 9.6. Unfortunately  $N(p)$  and  $N(T_e)$  also approach zero here, and we must study the slope of a continuously diminishing (and therefore statistically worsening) quantity of data.

The most attractive choice for an experimental measurement of this sort would be a decay with a small  $Q$  (so that the relative magnitude of the effect is larger) and one in which the atomic states before and after the decay are well understood, so that the important corrections for the influence of different atomic states can be calculated. (The effects of the atomic states are negligible in most  **$\beta$ -decay** experiments, but in this case in which we are searching for a very small effect, they become important.) The decay of  ${}^3\text{H}$  (tritium) is an appropriate candidate under both criteria. Its  $Q$  value is relatively small (18.6 keV), and the one-electron atomic wave functions are well known. (In fact, the calculation of the state of the resulting  ${}^3\text{He}$  ion is a standard problem in first-year quantum mechanics.) Figure 9.7 illustrates some of the more precise experimental results. Langer and Moffat originally reported an upper limit of  $m_\nu c^2 < 200$  eV, while two decades later, Bergkvist reduced the limit to 60 eV. One recent result may indicate a nonzero mass with a probable value between 14 and 46 eV, while others suggest an upper limit of about 20. Several experiments are currently being performed to resolve this question and possibly to reduce the upper limit.



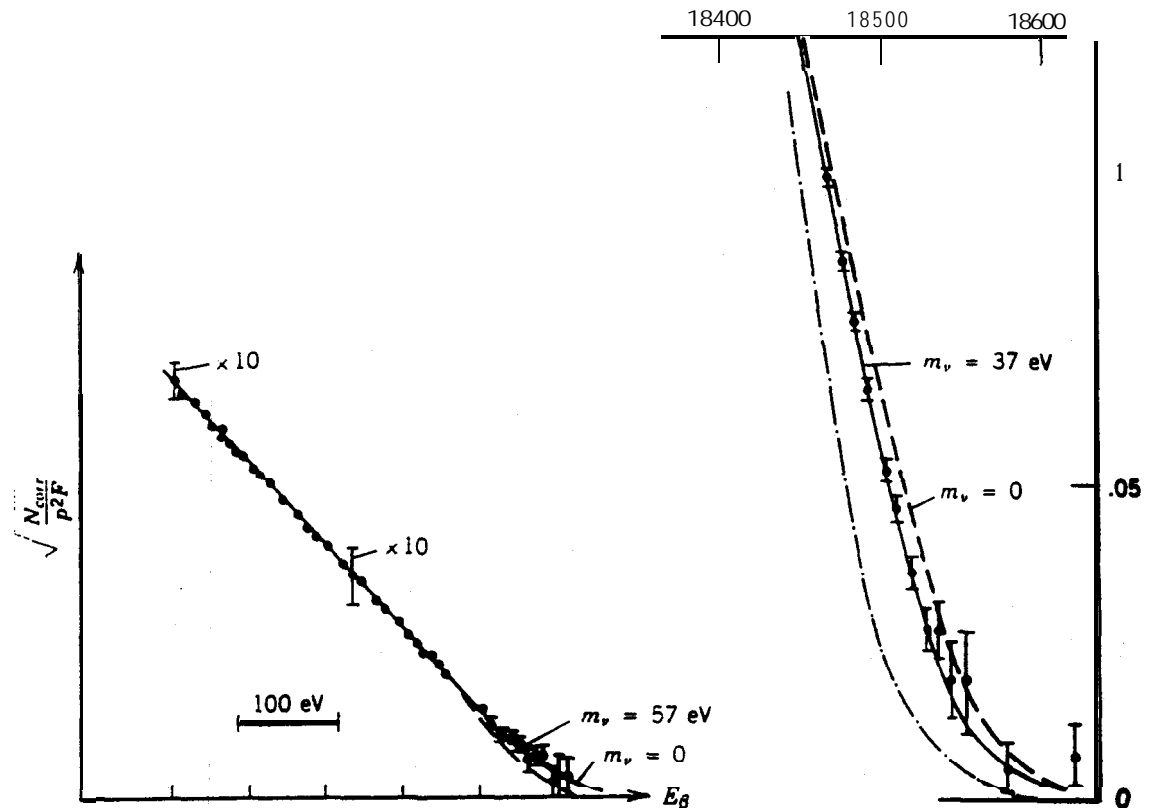


Figure 9.7 Experimental determination of the neutrino mass from the  $\beta$  decay of tritium ( $^3\text{H}$ ). The data at left, from K.-E. Bergkvist, *Nucl. Phys. B* 39, 317 (1972), are consistent with a mass of zero and indicate an upper limit of around 60 eV. The more recent data of V. A. Lubimov et al., *Phys. Lett. B* 94, 266 (1980), seem to indicate a nonzero value of about 30 eV; however, these data are subject to corrections for instrumental resolution and atomic-state effects and may be consistent with a vanishing mass.

Why is so much effort expended to pursue these measurements? The neutrino mass has very important implications for two areas of physics that on the surface may seem to be unrelated. If the neutrinos have mass, then the “electroweak” theoretical formalism which treats the weak and electromagnetic interaction as different aspects of the same basic force, permits electron-type neutrinos, those emitted in  $\beta$  decay, to convert into other types of neutrinos, called muon and tau neutrinos (see Chapter 18). This conversion may perhaps explain why the number of neutrinos we observe coming from the sun is only about one-third of what it is expected to be, based on current theories of solar fusion. At the other end of the scale, there seems to be more matter holding the universe together than we can observe with even the most powerful telescopes. This matter is nonluminous, meaning it is not observed to emit any sort of radiation. The Big Bang, cosmology, which seems to explain nearly all of the observed astronomical phenomena, predicts that the present universe should be full of neutrinos from the early universe, with a present concentration of the order of  $10^8/\text{m}^3$ . If these neutrinos were massless, they could not supply the necessary gravitational attraction to “close” the universe (that is, to halt and reverse the expansion), but with rest masses as low as 5 eV, they would provide sufficient mass-energy density. The study of the neutrino mass thus has direct and immediate bearing not only on nuclear and particle physics, but on solar physics and cosmology as